Low Complexity Iterative MLSE Equalization in Highly Spread Underwater Acoustic Channels

H.C. Myburgh
Dept. of Electrical, Electronic and Computer Engineering,
University of Pretoria
Pretoria, South Africa
herman.myburgh@up.ac.za

J.C. Olivier
Dept. of Electrical, Electronic and Computer Engineering,
University of Pretoria, and Defence Research, CSIR
Pretoria, South Africa
corne.olivier@eng.up.ac.za

***Abstract*—This work proposes a near-optimal hard output neural network based iterative Maximum Likelihood Sequence Estimation (MLSE) equalizer, based on earlier work by the authors, able to equalize single carrier 4-QAM signals in underwater acoustic channels with extremely long delay spreads. The performance of the proposed equalizer is compared to a suboptimal equalization technique, namely Decision Feedback Equalization (DFE), via computer simulation for a number of power delay profiles. Results show unparalleled performance at a fraction of the computational cost of optimal, yet impractical, equalization methods. The superior computational complexity of the proposed equalizer is due to the high parallelism and high level of neuron interconnection of its foundational neural network structure.**

I. Introduction

In recent years, much attention has been given to the equalization of underwater acoustic signals with long delay spreads. Due to the nature of the underwater acoustic channel (UAC), the inter-symbol interference (ISI) caused by multipath may extend over hundreds of symbols for moderate to high data rates, for single carrier systems. Also, the rapidly varying nature of the UAC introduces Doppler shifts, resulting in a fast varying CIR, complicating equalization even more [1].

Many equalization techniques for signals in the doubly dispersive UAC have been proposed over the last two decades [2]. Due to the high delay spread encountered in the UAC, classic equalization algorithms such as the Viterbi (VA) [3], [4] and Maximum A Posteriori Probability (MAP) [5] algorithms are practically infeasible, as their computational complexities are exponentially related to the number of interfering symbols, rendering them computationally infeasible for UAC equalization. Attention has therefore been drawn to developing computationally efficient equalization techniques at the cost of BER performance. Various single carrier DFE based techniques have been developed, where symbol-by-symbol decisions are made and fed back to be used in the next decision phase [6]. Although these techniques provide some performance improvement, the decision-and-feedback process causes noise enhancement, resulting in sub-optimal equalization.

As in the case of mobile wireless communication systems, multi-carrier (MC) modulation techniques, such as orthogonal frequency division multiplexing (OFDM) [7], have also been proposed for use in the UAC. The rationale behind using multi-carrier techniques is to increase the symbol period in order to alleviate the detrimental effects of ISI on the transmitted signal, facilitating trivial equalization complexity. Even when ISI cannot be eliminated completely, less ISI will ease the effort of equalization in each subcarrier. However, the use of MC signals in the UAC is not flawless. If the symbol interval is increased, it necessitates a corresponding decrease in the carrier spacing in order to adhere to the data rate and bandwidth conditions and restrictions. Decreased carrier spacing will render the system more susceptible to UAC-inherent Doppler shifts, resulting in inter-carrier interference (ICI) which will inevitably lead to degraded system performance [2].

Evidently there are a number of challenges to overcome in order to design an equalizer for a spectrally efficient underwater communication system. In summary: For single carrier systems, because there can be hundreds of interfering symbols, the symbol period can be increased to reduce the ISI span, leading to computationally efficient optimal equalization, while reducing the data rate and hence the spectral efficiency of the systems. Also, in MC systems, increasing the symbol period requires a corresponding reduction in the carrier spacing if the spectral efficiency is to be preserved, which will result in ICI due to Doppler shifts. The efficient transfer and detection of data in acoustic communication systems is therefore a difficult task due to the doubly spread nature of the UAC.

In this paper a near-optimal hard output Hopfield Neural Network (HNN) [8] based iterative MLSE equalizer is proposed to equalize single carrier 4-QAM modulated signals in a highly spread UAC. The proposed equalizer has computational complexity linear in the data block length and approximately independent from the CIR length, whereas conventional optimal equalizers have complexity linear in the data block length but exponential in the CIR length. Due to the high level of neuron interconnection and the parallelism of the single-layer recurrent neural network that forms the basis of this equalizer, it is able to effectively mitigate the effects of ISI caused by hundreds of interfering symbols, with relatively small computational cost. The performance of the proposed equalizer is compared to that of a DFE, for different delay spread profiles, and the results show that the proposed equalizer greatly outperforms the DFE. The computational complexity

1-4244-2523-5/09/$20.00 ©2009 IEEE

of the proposed equalizer presented to emphasize its significant computational complexity.

The BPSK version of the proposed equalizer[1] was first proposed by the authors in [9] for the equalization of BPSK signals in wireless communication systems with extremely long delay spreads in mobile fading channels. It was shown that the equalizer in [9] was able to equalize BPSK signals with CIR lengths of 200 with near-optimality at a fraction of the computational cost of an optimal equalizer. This is a significant result. The near-constant computational complexity of the equalizer proposed in this paper is only twice that of the BPSK version proposed by the authors in [9].

This paper is organized as follows. The neural network based hard output iterative MLSE equalizer is presented in Section 2 while an optimization technique is presented in Section 3. Section 4 presents the computational complexity proposed equalizer. In Section 6 the performance of the proposed equalizer is evaluated for different power delay profiles and compared to the performance of the DFE. Conclusions are drawn in Section 7.

II. The iterative MLSE equalizer

To find the most probable transmitted sequence in a single carrier wireless communication systems, the cost function

$$\mathcal{L} = \sum_{k=1}^{N} \left| r_k - \sum_{j=0}^{L-1} h_j s_{k-j} \right|^2, \tag{1}$$

must be minimized [10]. Here N is the data block length, L is the CIR length, r_k denotes the kth received symbol, s_{k-j} denotes the $(k-j)$th most likely transmitted symbol, h_j is the jth coefficient of the estimated CIR, assumed to be time-invariant for a given data block, and n_k is the kth Gaussian noise sample $\mathcal{N}(0, \sigma^2)$. The Viterbi MLSE equalizer [10] is able to minimize (1) in order to produce the maximum likelihood sequence of transmitted symbols $\mathbf{s} = \{s_1, s_2, \cdots, s_N\}^T$, where ^{T} denotes the transpose operation. However, the computational complexity involved in solving this problem exactly, scales linearly with an increase in N and exponentially with an increase in L, therefore rendering the problem infeasible for systems with large L.

Any algorithm used to perform MLSE equalization in a single carrier wireless communication systems must therefore be able to minimize (1). The proposed iterative MLSE equalizer minimizes (1) to find the most probable transmitted sequence with near-optimality at very low computational cost.

A. System Model

By expanding (1) and ignoring the exponential terms [2] (1) can be written in the form

$$\mathcal{L} = -\frac{1}{2}\mathbf{s}^\dagger \mathbf{T}\mathbf{s} - \mathbf{I}^\dagger \mathbf{s}, \tag{2}$$

where $\mathbf{I}$ is a column vector with N elements, $\mathbf{T}$ is a square correlation matrix of size N, and † denotes the Hermitian transpose. The cost function in (2) is in the exact form of the HNN proposed in [8], that was demonstrated to solve various optimization problems, among which were the well-know traveling salesperson problem (TSP) and analog-to-digital (A/D) conversion. Therefore, by expanding (1) and mapping it to (2), the problem of MLSE equalization can be solved with the use of the HNN, given $\mathbf{T}$ and $\mathbf{I}$ in (2). Systematic derivationsof $\mathbf{T}$ and $\mathbf{I}$ are presented in the next section.

For systems employing M-QAM modulation schemes, (2) needs some treatment to account for the complex terms. Therefore the variables in (2) must be adapted as follows:

$$\begin{aligned} \mathbf{u} &= [\mathbf{u}_i^T | \mathbf{u}_q^T], \\ \mathbf{s} &= [\mathbf{s}_i^T | \mathbf{s}_q^T], \\ \mathbf{I} &= [\mathbf{I}_i^T | \mathbf{I}_q^T], \\ \mathbf{T} &= \begin{bmatrix} \mathbf{X}_i & \mathbf{X}_q^T \\ \mathbf{X}_q & \mathbf{X}_i \end{bmatrix}, \end{aligned}$$

where $\mathbf{s}_i$ and $\mathbf{s}_q$ denote the respective real and complex sequence estimate component vectors, $\mathbf{X}_i$ and $\mathbf{X}_q$ are symmetrics square matrices of size N, and $\mathbf{I}_i$ and $\mathbf{I}_q$ are vectors with N elements.

1) Systematic derivation: When (1) is expanded, for CIR lengths from $L = 2$ to $L = 6$, and mapped to (2) for each case, a pattern emerges in $\mathbf{X}_i$, $\mathbf{X}_q$, $\mathbf{I}_i$, and $\mathbf{I}_q$. By following the logic of the pattern, $\mathbf{X}_i$, $\mathbf{X}_q$, $\mathbf{I}_i$, and $\mathbf{I}_q$ can be determined for the general case. For an M-QAM (M-arry Quadrature Amplitude Modulation) system $\mathbf{X}_i$ is given by

$$\mathbf{X}_i = -\begin{bmatrix} 0 & \alpha_1 & \dots & \alpha_{L-1} & \dots & 0 \\ \alpha_1 & 0 & \alpha_1 & \dots & \ddots & \vdots \\ \vdots & \alpha_1 & 0 & \ddots & \vdots & \alpha_{L-1} \\ \alpha_{L-1} & \vdots & \ddots & \ddots & \alpha_1 & \vdots \\ \vdots & \ddots & \dots & \alpha_1 & 0 & \alpha_1 \\ 0 & \ddots & \alpha_{L-1} & \dots & \alpha_1 & 0 \end{bmatrix} \tag{3}$$

where $\alpha = \{\alpha_1, \alpha_2, \cdots, \alpha_{L-1}\}$ is determined by

$$\alpha_k = \sum_{j=0}^{L-k-1} h_{i,j} h_{i,j+k} + \sum_{j=0}^{L-k-1} h_{q,j} h_{q,j+k}, \tag{4}$$

where $k = 1, 2, 3, ..., L-1$ and i and j denote the real and complex components of the CIR coefficients. Similarly $\mathbf{X}_q$ is given by

[1] The proposed 4-QAM equalizer is an extension of the one proposed in [9].

[2] This step is valid, since the exponetial terms only provide a positive offset to the cost of (1).

$$\mathbf{X}_q = -\begin{bmatrix} 0 & \gamma_1 & \dots & \gamma_{L-1} & \dots & 0 \\ \gamma_1 & 0 & \gamma_1 & \dots & \ddots & \vdots \\ \vdots & \gamma_1 & 0 & \ddots & \vdots & \gamma_{L-1} \\ \gamma_{L-1} & \vdots & \ddots & \ddots & \gamma_1 & \vdots \\ \vdots & \ddots & \dots & \gamma_1 & 0 & \gamma_1 \\ 0 & \ddots & \gamma_{L-1} & \dots & \gamma_1 & 0 \end{bmatrix} \quad (5)$$

where $\gamma = \{\gamma_1, \gamma_2, \cdots, \gamma_{L-1}\}$ is determined by

$$\gamma_k = \sum_{j=0}^{L-k-1} h_{q,j} h_{i,j+k} - \sum_{j=0}^{L-k-1} h_{i,j} h_{q,j+k}, \quad (6)$$

where again $k = 1, 2, 3, ..., L-1$ and i and j denote the real and complex components of the CIR coefficients. Also,

$$\mathbf{I}_i = \begin{bmatrix} \sum_{j=0}^{L-1} r_{i,j+1} h_{i,j} + \sum_{j=0}^{L-1} r_{q,j+1} h_{q,j} \\ \sum_{j=0}^{L-1} r_{i,j+2} h_{i,j} + \sum_{j=0}^{L-1} r_{q,j+2} h_{q,j} \\ \sum_{j=0}^{L-1} r_{i,j+3} h_{i,j} + \sum_{j=0}^{L-1} r_{q,j+3} h_{q,j} \\ \vdots \\ \vdots \\ \sum_{j=0}^{L-1} r_{i,j+(N-2)} h_{i,j} + \sum_{j=0}^{L-1} r_{q,j+(N-2)} h_{q,j} \\ \sum_{j=0}^{L-1} r_{i,j+(N-1)} h_{i,j} + \sum_{j=0}^{L-1} r_{q,j+(N-1)} h_{q,j} \\ \sum_{j=0}^{L-1} r_{i,j+N} h_{i,j} + \sum_{j=0}^{L-1} r_{q,j+N} h_{q,j} \end{bmatrix} \quad (7)$$

and

$$\mathbf{I}_q = \begin{bmatrix} \sum_{j=0}^{L-1} r_{q,j+1} h_{i,j} - \sum_{j=0}^{L-1} r_{i,j+1} h_{q,j} \\ \sum_{j=0}^{L-1} r_{q,j+2} h_{i,j} - \sum_{j=0}^{L-1} r_{i,j+2} h_{q,j} \\ \sum_{j=0}^{L-1} r_{q,j+3} h_{i,j} - \sum_{j=0}^{L-1} r_{i,j+3} h_{q,j} \\ \vdots \\ \vdots \\ \sum_{j=0}^{L-1} r_{q,j+(N-2)} h_{i,j} - \sum_{j=0}^{L-1} r_{i,j+(N-2)} h_{q,j} \\ \sum_{j=0}^{L-1} r_{q,j+(N-1)} h_{i,j} - \sum_{j=0}^{L-1} r_{i,j+(N-1)} h_{q,j} \\ \sum_{j=0}^{L-1} r_{q,j+N} h_{i,j} - \sum_{j=0}^{L-1} r_{i,j+N} h_{q,j} \end{bmatrix}, \quad (8)$$

provided that the $L-1$ tail symbols added to both sides of the data block are equal to $0 + j0$.

2) Training: Since the proposed iterative MLSE equalizer is based on a neural network, it has to be trained. The neural network is trained for every received data block, by using the coefficients of the the estimated CIR. Therefore, $\mathbf{X}_i$, $\mathbf{X}_q$, $\mathbf{I}_i$, and $\mathbf{I}_q$ fully described the structure of the equalizer for each received data block. $\mathbf{X}_i$ and $\mathbf{X}_q$ describe the connection weights between the neurons, and $\mathbf{I}_i$ and $\mathbf{I}_q$ represent the bias input of the neural network.

B. Iterative MLSE Equalization

To minimize (2) in order to obtain the MLSE estimate of the transmitted symbols $\mathbf{s}$, (2) is differentiated with respect to $\mathbf{u}$. This leads to the dynamic system

$$\frac{d\mathbf{u}}{dt} = -\frac{\mathbf{u}}{\tau} + \mathbf{T}\mathbf{s} + \mathbf{I}, \quad (9)$$

where τ is an arbitrary constant and $\mathbf{u} = \{u_1, u_2, \cdots, u_N\}^T$, which can be iterated to find the MLSE estimated $\mathbf{s}$.

It was shown in [8] that (2) is a Lyapunov function where $\beta \to \infty$ for the dynamic system in (9). By definition of a Lyapunov function, this system is guaranteed to converge to a steady state $\mathbf{u}$ so that $\mathbf{s}$ will minimize the cost function in (2). $\mathbf{s}$ is therefore the MLSE sequence estimate.

An iterative solution for (9) is given by

$$\begin{aligned} \mathbf{u}^{(n+1)} &= \mathbf{T}\mathbf{s}^{(n)} + \mathbf{I} \\ \mathbf{s}^{(n+1)} &= g(\beta^{(n+1)}\mathbf{u}^{(n+1)}) \end{aligned} \quad (10)$$

where n indicates the iteration number and $g(\beta u_k)$, where the gain $\beta = 1$, is a bipolar decision function. The system is iterated until the system energy converges to a minimum, after which the MLSE estimates are presented in $\mathbf{s}$.

III. Annealing

β is updated for each iteration cycle according to

$$\beta^{(n)} = 5^{\frac{2(n-Z+1)}{Z}}, \quad (11)$$

shown in Fig. 1, where *Z* indicates the number of iterations and *n* denoted the iteration number. This causes β to start at a near-zero value and to exponentially converge to 1 with each iteration. This process is called simulated annealing, and it enables the system to escape less optimal local minima in the solution space. The effect of annealing on the neurons during the iteration cycle is shown in Fig. 2, with the slope of the sigmoid function increasing with each iteration. From Fig. 3 it is clear that the use of annealing on the neurons minimizes the energy of the system more effectively, therefore achieving better performance.

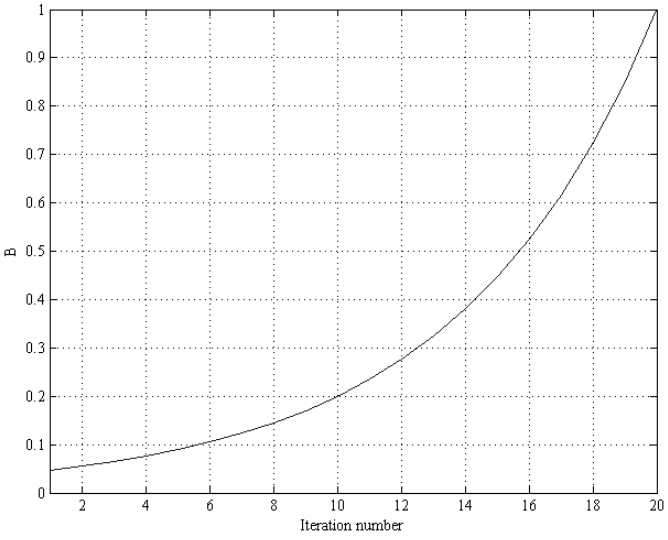

Fig. 1. β-updates for $Z = 1$ to $Z = 20$.

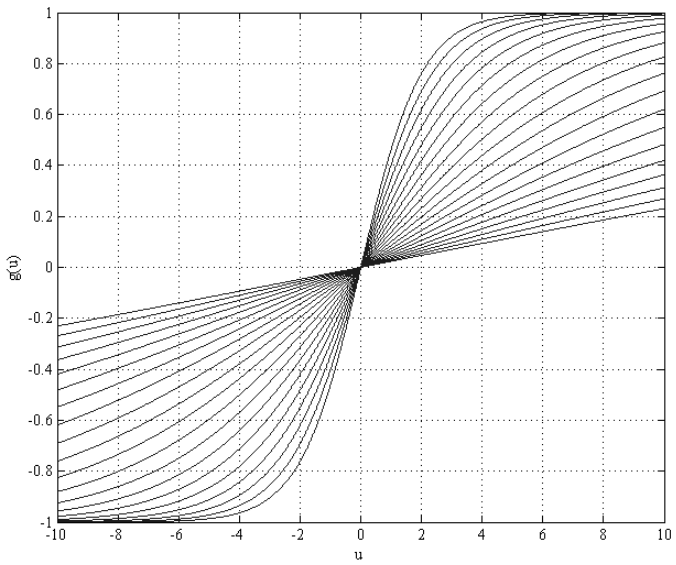

Fig. 2. Simulated annealing updates for $Z = 1$ to $Z = 20$.

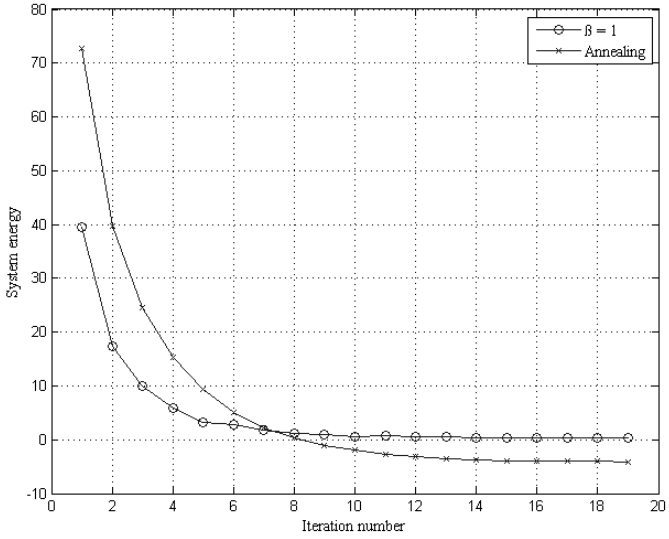

Fig. 3. Energy minimization for $Z = 1$ to $Z = 20$.

IV. Computational complexity

For an M-QAM system with with $M > 2$, a block of N transmitted symbols $\mathbf{s} = \{s_1, s_2, \cdots, s_N\}$, a CIR length L, and Z iterations,[3] the computational complexity[4] of the proposed MLSE equalizer is $4ZN(N+3)+8L(N+1)+2L^2$. [5] The Viterbi MLSE equalizer has computational complexity $\propto NM^{(L-1)}$. Fig. 4 shows the computational complexity of the proposed equalizer for $L = 2$ to $L = 1000$ for a data block length of $N = 1200$.

[3] $Z = 20$ iterations are used per data block

[4] The computational complexity of an M-QAM iterative equalizer is independent of the number of symbols in the modulation alphabet for $M > 2$.

[5] For $N >> L$ the effect of L becomes negligible.

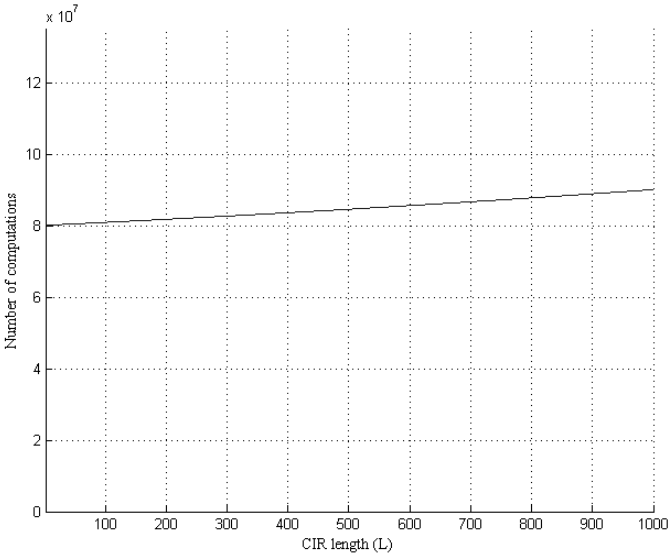

Fig. 4. Computational complexity for $L = 2$ to $L = 1000$.

For communication systems with large delay spreads, as in the case of UACs, the computational complexity of the proposed equalizer is almost independent of the CIR length L. This allows the proposed MLSE equalizer to equalize ISI-corrupted signals in systems with hundreds of interfering symbols near-optimally with relative ease. The significant computational complexity of the proposed equalizer is due to the high parallelism of its underlying neural network structure and the high level of interconnection of the neurons.

V. Simulation

The proposed iterative MLSE equalizer was evaluated for different modulation schemes and for different channel delay profiles. All simulation where carried out for a carrier frequency f_c = 15 kHz with symbol interval of T_s = 50 μs, for various CIR lengths from $L = 50$ to $L = 1000$, corresponding to delay spreads of 2.5 ms to 50 ms, with a data block length of $N = 1200$ symbols and a Doppler frequency of F_D = 5 Hz.[6] $L-1$ known tail symbols were appended and prepended to the data block. Also, to simulate the fading effect of each tap, the Rayleigh fading simulator proposed in [11] was used to generate uncorrelated fading vectors. Perfect channel state information (CSI) was assumed, by using the center value of each fading vector to construct the CIR for each data block.

A. Power Delay Profiles

Three different power dealy profiles were used to characterize the channel delay spread in the UAC. The nominal CIR weights[7] were chosen as $\mathbf{h} = \{\frac{h_0}{\|\mathbf{h}\|}, \frac{h_1}{\|\mathbf{h}\|}, \cdots, \frac{h_{L-1}}{\|\mathbf{h}\|}\}$ such that $\mathbf{h}^T\mathbf{h} = 1$, where L is the CIR length, and $\mathbf{h}$ is a column vector of length L. After normalization, the coefficients of $\mathbf{h}$

[6] Although the simulations were performed in baseband, the settings of f_c, T_s, and F_D were used to generate realistic Rayleigh fading vectors.

[7] The coefficients of $\mathbf{h}$ are determined by the power delay profile.

were used to scale the respective Rayleigh fading vectors used to simulate the multipath effect, in order to produce realistic UAC simulation results. The power delay profile models are described in turn below:

1) Exponential decay: The exponential decaying power delay profile coefficients are determined by

$$h_k = exp\Big(\frac{-k\tau_{max}}{L\tau_e}\Big) \tag{12}$$

where $k = 0, 1, 2, ..., L-1$, τ_{max} is the channel delay spread duration, and τ_e is the time constant of the profile, determined by

$$\tau_e = \frac{-\tau_{max}}{ln\Big(10^{\frac{P_{drop}}{10}}\Big)}, \tag{13}$$

where P_{drop} is the relative power drop between $t = 0$ and $t = \tau_{max}$, with a value of -30 dB. The normalized exponential power delay profile coefficients are shown in Fig. 5 for $L = 50$.

2) Linear decay: The linear decaying power delay profile coefficients are determined by

$$h_k = \frac{L-k}{L}. \tag{14}$$

where $k = 0, 1, 2, ..., L-1$. The normalized linear power delay profile is shown in Fig. 6 for $L = 50$.

3) Random decay: The random decaying power delay profile coefficients are determined by

$$h_k = Random(), \tag{15}$$

where $k = 0, 1, 2, ..., L-1$ and the function $Random()$ generates uniformly distributed random numbers such that $h_k \in [0; 1]$. Fig. 7 shows a normalized random power delay profile for $L = 50$.

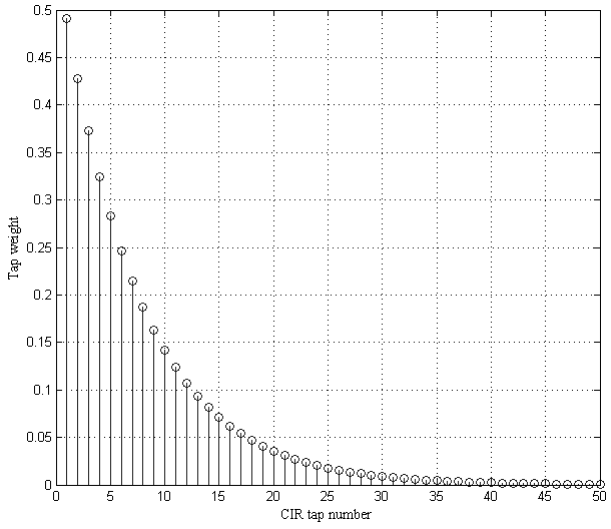

Fig. 5. Exponential power delay profile for $L = 50$.

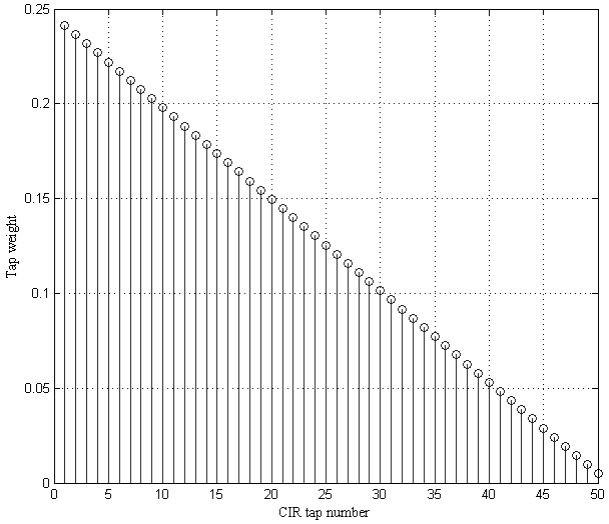

Fig. 6. Linear power delay profile for $L = 50$.

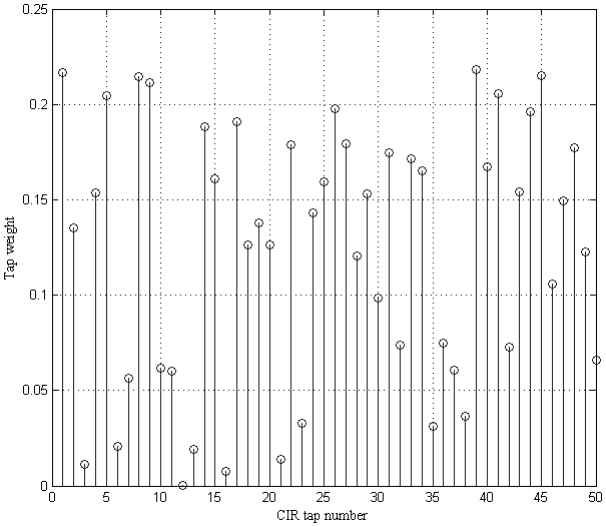

Fig. 7. Random power delay profile for $L = 50$.

B. Numerical Results

The proposed iterative MLSE equalizer was simulated for the exponential-, random- , and linear channel delay profiles, for 4-QAM modulation, in a frequency-selective Rayleigh fading environment. Frequency hopping was employed, by generating unique uncorrelated fading vectors for each fading channel, for each transmitted data block, to improve system performance. CIR lengths of $L = 50$ to $L = 1000$, corresponding to channel delays of 2.5 ms to 50 ms, were evaluated. Fig. 8 to Fig. 12 show the 4-QAM performance of the proposed iterative MLSE equalizer. It is clear that the proposed MLSE equalizer effectively equalizes the ISI-corrupted received symbols for systems with extremely long CIR lengths, recombining the signal energy spread by the UAC among the channels. The performance of the equalizer

is lowest for the exponential decaying power delay profile, since most of the signal energy is concentrated in the first few taps of the CIR. However, when the linear- and random power delay profiles are considered, the performance improves significantly, indicating that the proposed equalizer performs well when the signal energy is spread among the CIR taps.

Fig. 13 to Fig. 15 show the performance of the proposed equalizer for CIR lengths from $L = 50$ to $L = 1000$ for the exponential-, random-, and linear power delay profiles, compared to the performance of a non-adaptive DFE in each case. The proposed iterative MLSE equalizer clearly outperforms the DFE, as it is able to effectively recombine the ISI-corrupted received symbols, producing near-optimal estimates of the original transmitted symbols.

These results confirm that the proposed iterative MLSE equalizer is able to equalize signals in systems where the transmitted signal is corrupted by hundreds of interfering symbols, a phenomenon that is prevalent in underwater communication systems. The error floors observed in the simulation results are due to inaccurate CIR estimates caused by the time varying nature of the UAC during the transmission of one data block, becoming more severe as the Doppler frequency increases.

VI. Conclusion

In this work a low complexity neural network based iterative MLSE equalizer was proposed, with computational complexity linear in the data block length and approximately independent of the CIR length. This approximated independence enables the it to equalize signals in UACs with hundreds of multipath elements, as the dominant term in the computational complexity of conventional equalization algorithms is the CIR length L. The proposed MLSE equalizer can be extended to enable the equalization of any M-QAM signal constellation, without an increase in the computational complexity.[8] Conventional equalizers rely heavily on linearization techniques to alleviate the computational strain, but the high parallelism of the underlying neural network structure of the proposed equalizer, together with the high level of interconnectivity of its neurons, enable nonlinear equalization at a fraction of the computational complexity of conventional optimal equalizers. The proposed iterative MLSE equalizer is therefore a major step forward in the field of single carrier MLSE equalization in highly spread UACs.

References

[1] J.C. Preisig L. Weichang. "Estimation and Equalization of Rapidly Varying Sparse Acoustic Communication Channels". *Oceans 2006*, pages 1–6, 2006.

[2] M. Stojanovic. *"Acoustic Communications" in Encyclopedia of Telecommunications*. John Wiley and Sons, 2003.

[3] A.D. Viterbi. "Error bounds for convolutional codes and an asymptotically optimum decoding algorithm". *IEEE Transactions on Information Theory*, IT–13(1):260–269, 1967.

[4] J.G. Proakis. *Digital Communications*. McGraw-Hill, International Edition, New York, 4 th edition, 2001.

[5] L. Bahl, J. Cocke, F. Jelinek, and J. Raviv. "Optimal decoding of linear codes for minimizing symbol error rate". *IEEE Transactions on Information Theory*, IT-20:284–287, March 1974.

[6] L. Freitag M. Stojanovic and M. Johnson. "Channel Estimation Based Adaptive Equalization of Underwater Acoustic Signals". *Oceans 1999*, 2:985–990, 1999.

[7] J. Terry and J. Heiskala. *OFDM Wireless LANs: A Theoretical and Practical Guide*. Sams Publishing, Indianapolis, IN, 2001.

[8] J.J. Hopfield and D.W. Tank. "Neural computations of decisions in optimization problems". *Biology and Cybernetics*, 52:1–25, 1985.

[9] H.C. Myburgh and J.C. Olivier. "Near-Optimal Low Complexity MLSE Equalisation". *Wireless Communications and Networking Conference*, WCNC 2008:226–230, 2008.

[10] G.D. Forney. "The Viterbi Algorithm". *Proceedings of the IEEE*, 61(3):268–278, March 1973.

[11] Y.R. Zheng and C. Xiao. "Improved models for the generation of multiple uncorrelated Rayleigh fading waveforms". *IEEE Commununications Letters*, 6:256–258, June 2002.

[8] A 16-QAM equalizer was successfully developed. It produces equally spectacular results.

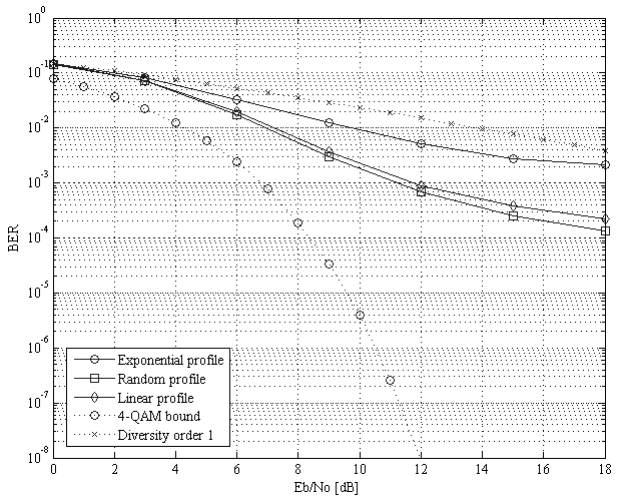

Fig. 8. 4-QAM performance for all power delay profiles for $L = 50$.

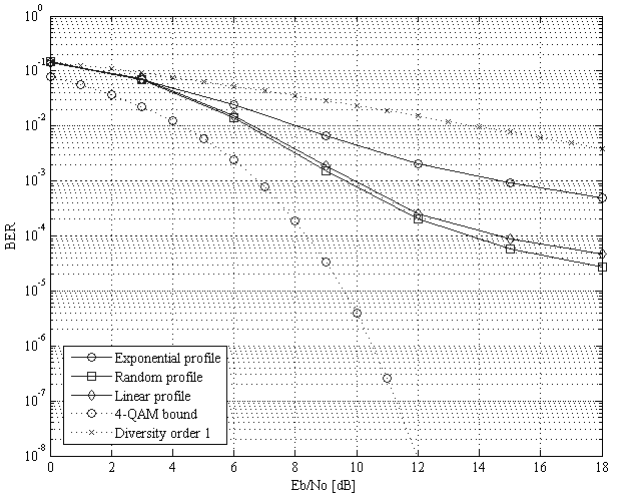

Fig. 9. 4-QAM performance for all power delay profiles for $L = 100$.

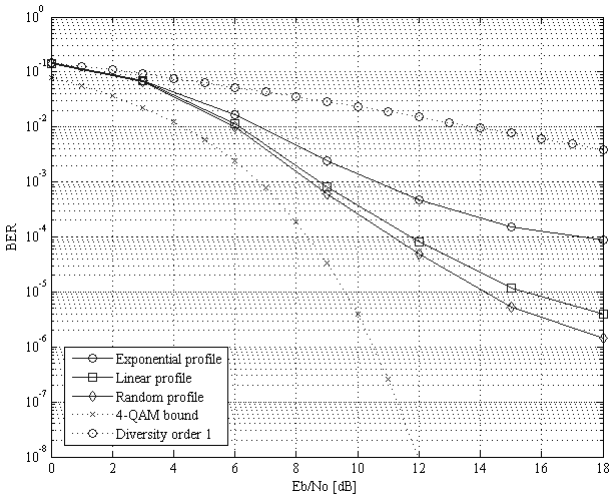

Fig. 10. 4-QAM performance for all power delay profiles for $L = 250$.

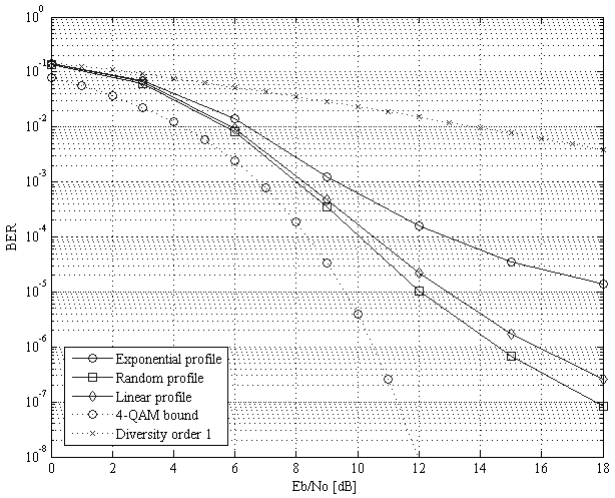

Fig. 11. 4-QAM performance for all power delay profiles for $L = 500$.

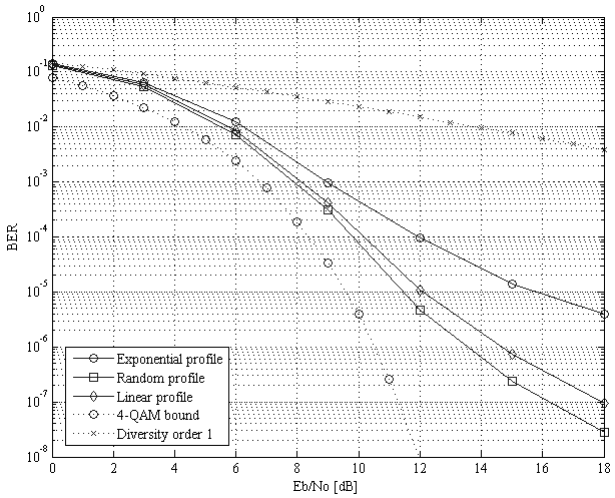

Fig. 12. 4-QAM performance for all power delay profiles for $L = 1000$.

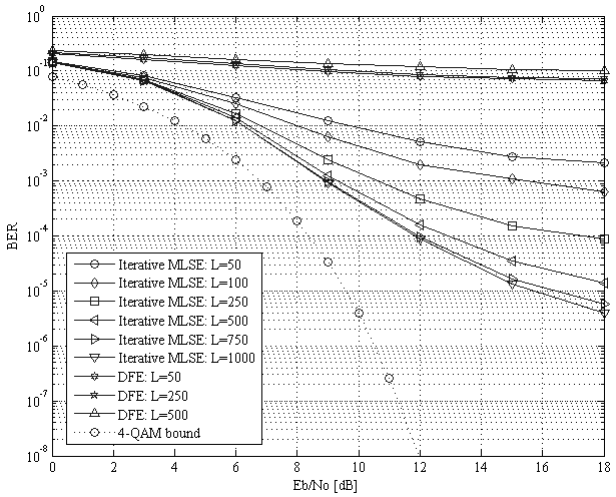

Fig. 13. 4-QAM performance for the exponential power delay profile.

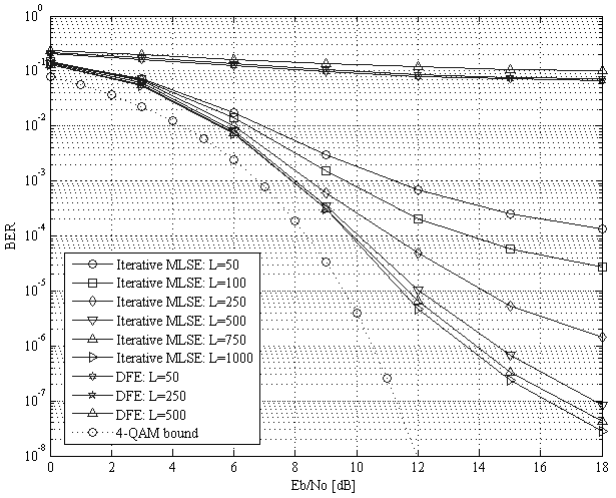

Fig. 14. 4-QAM performance for the random power delay profile.

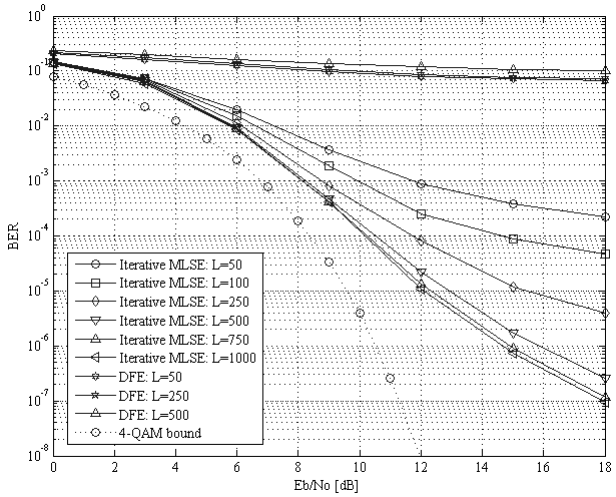

Fig. 15. 4-QAM performance for the linear power delay profile.